SHORT REFERENCE IMAGE QUALITY RATING BASED ON ANGULAR EDGE COHERENCE

L. Capodiferro[(*)], E. D. Di Claudio[(**)], and G. Jacovitti[(***)]

[(*)]Fondazione "U. Bordoni"
Via Baldassarre Castiglione 59, I-00142, Rome, Italy
phone: + (39) 06 54802132, fax: + (39) 54804405, email: lcapodiferro@fub.it
web: http\\www.fub.it
[(**)(***)]INFOCOM Dpt., University of Rome "La Sapienza"
Via Eudossiana 18, I-00184, Rome, Italy
[(**)] phone: + (39) 06 44585490, fax: + (39) 06 4873300, email: dic@.infocom.uniroma1.it
[(***)] phone: + (39) 06 44585838, fax: + (39) 06 4873300, email: gjacov@infocom.uniroma1.it
[(**)(***)] web: http:\\infocom.uniroma1.it

ABSTRACT

A very concise comparison technique for objective image quality assessment is described. The method is based on a angular edge coeherence measure defined by local image expansion into a set of harmonic angular functions. Using the angular edge coherence it is possible to estimate the relative quality of a reproduced image with respect to the original one comparing only the values of a single statistical index disjointly extracted from each image. The present contribution briefly illustrates the mathematical support of this technique and provides some significant experimental examples.

1. GENERAL INFORMATION

Image quality is becoming a central factor in many applications ranging from TV broadcasting, personal mobile communication, medicine, security, remote sensing, scientific investigation, etc. For this reason, production, delivery and use of images requires today reliable automatic image quality assessment tools.

Automatic image quality classification is often performed by direct (pixel by pixel) comparison of the obtained images with the originals ones, using conventional signal metrics, such as MSE, SNR, PSNR etc. This is the so-called Full-Reference (FR) approach. To improve the correlation of objective measures with human subjective judgement, more sophisticated metrics have been designed to take into account quantifiable weigths provided by available (crude) mathematical models of the human visual system (HVS). Alternative approaches are based on structure-oriented comparison.

To minimize the side information necessary for quality assessment in telecommunication applications, some so-called Reduced Reference (RR) approaches compare selected features of the original image with the corresponding ones of the received one. Features are sent from the source to the user through auxiliary low-capacity channels. Examples of relatively parsimonious RR techniques, are presented in [1], [2] and [3].

In this contribution we present an extremely concise RR method, which requires transmission of a single number for feature comparison and subsequent quality assessment, corresponding to one ten bits. This brevity could be advantageously exploited for instance for inserting quality indicators directly in the image header section of streaming sequences. The method described here is based on a particular metric based on a properly defined structural coherence of edges. This metric, derived by image decomposition with the so-called Gauss-Laguerre (GL) family of angular harmonic functions, is sensitive to different quality impairment factors encountered in practice, as illustrated in the foregoing.

2. THE BASIC CONCEPT

The method is founded on two basic assumptions:

- The original and the observed image represent the same objects. As such, they share the same edge population.
- The visual quality of the image is strictly correlated to the structural coherence of edges. Such concepts are alredy present in the technical literature (see for instance [4]).

In particular, it is shown here that the local "angular edge coherence" (AEC), defined in the framework of the angular harmonic image decomposition, is corrupted at the same time by distortions (such as blur or deviations) and/or by disturbances (such as noise and artifacts). The local AEC is of particular interest because of its simplicity and its peculiar shift and rotation invariance property.

Based on above assumptions, weigthed averages of the local AEC values independently calculated on the original image and on the observed one are compared. The ratio of the these statistics measures the *relative* quality of the latter one with respect to the former one.

To illustrate how these concepts are formally stated and how effective the assumptions are, let us first briefly introduce the basic mathematical support.

2.1 Image decomposition

Let us locally represent the original image image $\tilde{I}(x_1, x_2)$ and the observed one $I(x_1, x_2)$, both defined on the the coordinates x_1, x_2 of the real plane $\mathbb{R}^2$, by the Gauss-Laguerre (GL) functions [5]. GL functions form a complete orthogonal family under a Gaussian weigth. In the polar coordinates $r = \sqrt{x_1^2 + x_2^2}$, $\gamma = tg^{-1}\{x_2 / x_1\}$ they have the general expression:

$$\mathcal{L}_k^{(n)}(r/\sigma, \gamma) = P_{k,n} g(r/\sigma)_{k,n} e^{jn\gamma}$$

where:

$$P_{k,n} = (-1)^k 2^{(|n|+1)/2} \pi^{|n|/2} \left[\frac{k!}{(|n|+k)!} \right]^{1/2}$$

$$g(r/\sigma)_{k,n} = (r/\sigma)^{|n|} L_k^{(|n|)}\left(2\pi (r/\sigma)^2\right) e^{-\pi (r/\sigma)^2}$$

$L_k^{(n)}$ are the generalized Laguerre polynomials of order n, k. σ and is a scale factor. These functions $L_k^{(n)}(r, \gamma)$ are polar separable, with radial profile $g\left(r/\sigma\right)$ and angular modulation $e^{jn\gamma}$. GL functions possess remarkable mathematical properties. Among others, they are "*self steering*", i.e. a plane rotation by the angle α shifts the phase of the *n*-th order functions by the angle $n\alpha$.

GL coefficients are calculated by convolutions. Passing the image $I(x_1, x_2)$, through a filter having impulse response $\mathcal{L}_k^{(n)}\left(r/\sigma, \gamma\right)$ yields an image $Y_{k,n}(x_1, x_2)$ which is the (complex) map of the GL coefficients of order n, k.

The series of coefficients $Y_{k,n}(x_1', x_2')$ of the image windowed around the point (x_1', x_2') defines a local spectrum similar to the classical Fourier-Mellin transform. For patterns characterized by sharp variations the series converges slowly, whereas smooth patterns are characterized by few significant coefficients.

Interesting enough, the phase relationship among GL coefficients is related to the underlying pattern structure. Such relationship is easily understood by analogy with the windowed Fourier transform for a monodimensional signal. Here, the spectrum phase is indicative of some general features of the windowed signal. For instance, symmetric patterns have generalized zero phase, whereas random patterns have random phase. By analogy, it is easily shown that the phase of the GL spectrum in a window centered on an *ideal edge pattern* presents non zero coefficients only for even values of n, with linear phase versus n (except for π phase jumps). The initial phase, for $n = 1$, indicates the direction orthogonal to the edge (maximum gradient direction). In a quite similar fashion, it is shown that the GL spectrum in a window centered on a *line pattern* presents non zero coefficients for odd n, with linear phase versus n (except for π jumps).

3. THE ANGULAR EDGE COHERENCE

These basic properties do suggest that the local GL expansion can be employed for measuring how much edges and lines of an image are distorted and/or affected by disturbances. Since degradations of edges and lines are usually strictly related each other, let us focus here our attention only on edges. In particular, let us consider the GL coefficients for $k = 0$ and $n = 1$, and $n = 3$ of the original image $\tilde{I}(x_1, x_2)$ in the correspondence of an ideal edge pattern point $(\bar{x}_1, \bar{x}_2)$. The Fourier spectra of the impulse responses of the employed GL filters are displayed in Fig.1

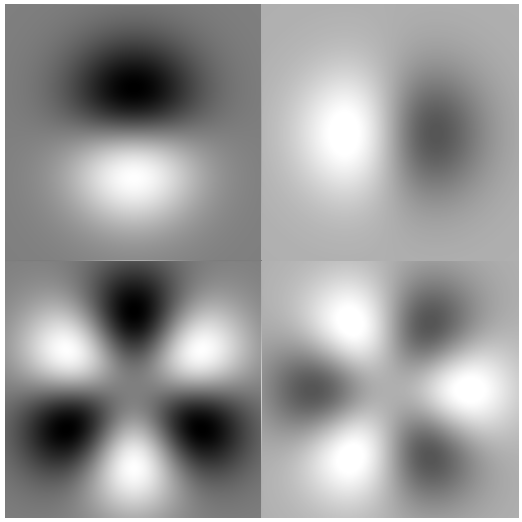

Figure 1: Real part (left) and imaginary part (right) of theFourier transform of the GL functions for $k = 0$ $n = 1$ (top) and $n = 3$ (bottom).

The impulse responses of the GL filters have exactly the same shape of their Fourier transforms, with different scale and orientation.

It is shown that, for $(\bar{x}_1, \bar{x}_2)$ exactly centered on *ideal* edges:

$$\frac{\left|\tilde{Y}_{0,n}(\bar{x}_1, \bar{x}_2)\right|}{\left|\tilde{Y}_{0,1}(\bar{x}_1, \bar{x}_2)\right|} = \frac{1}{2}$$

When edges are not ideal, and elsewhere in the plane, the above harmonic magnitude ratio is mostly smaller.

In addition, the relationship between the phase $\tilde{\varphi}_{01}(\bar{x}_1, \bar{x}_2)$ of $\tilde{Y}_{0,1}(\bar{x}_1, \bar{x}_2)$ and $\tilde{\varphi}_{03}(\bar{x}_1, \bar{x}_2)$ of $\tilde{Y}_{0,3}(\bar{x}_1, \bar{x}_2)$ is

$$\tilde{\varphi}_{03}(\bar{x}_1, \bar{x}_2) = 3\tilde{\varphi}_{01}(\bar{x}_1, \bar{x}_2) + \pi$$

or equivalently,

$$\mathrm{Re}\left[e^{j(\tilde{\varphi}_{03}(\bar{x}_1, \bar{x}_2) - 3\tilde{\varphi}_{01}(\bar{x}_1, \bar{x}_2))}\right] = -1$$

For non ideal edges, and elsewhere in the plane, the above quantity varies in the range. (–1, +1).

Based on these properties, let us formally introduce now the *angular edge coherence (AEC)* function for any point of the

plane for the original image and for the observed one, defined as:

$$\frac{\left|\tilde{Y}_{0,3}(x_1,x_2)\right|}{\left|\tilde{Y}_{0,1}(x_1,x_2)\right|}\mathrm{Re}\left[e^{j\tilde{\varphi}_{03}(x_1,x_2)}\cdot e^{-j3\tilde{\varphi}_{01}(x_1,x_2)}\right]$$

$$\frac{\left|Y_{0,3}(x_1,x_2)\right|}{\left|Y_{0,1}(x_1,x_2)\right|}\mathrm{Re}\left[e^{j\varphi_{03}(x_1,x_2)}\cdot e^{-j3\varphi_{01}(x_1,x_2)}\right]$$

The above function possesses two remarkable properties: it is translation and *rotation* invariant, owing to the cited self-steering property of the GL basis.

Then, the *total angular edge coherence* (TAEC) of the image $\tilde{I}(x_1,x_2)$ is defined as the following statistical mean:

$$TAEC\left(\tilde{I}\right)=\frac{1}{N}\sum\left\{\left|\tilde{Y}(x_1,x_2)_{0,1}\right|\left|\tilde{Y}_{0,3}(x_1,x_2)\right|\times R\mathrm{e}\left[e^{j\tilde{\varphi}_{03}(x_1,x_2)}e^{-j3\tilde{\varphi}_{01}(x_1,x_2)}\right]\right\}$$

where edge features are weighted by the edge strength factor $\left|\tilde{Y}(x_1,x_2)_{0,1}\right|^2$.

Here and in the subsequent formulas Σ indicates summation of N samples on the x_1,x_2 plane. In our experiments, the whole grid of available pixels is scanned, committing the role of (soft) edge extractor to the weighting factor $\left|\tilde{Y}(x_1,x_2)_{0,1}\right|^2$. In the same obvious way we define the TAEC of the observed image $TAEC(I)$.

It is expected that the TAEC is relatively large for good quality natural images. This expectation is justified by the fact that natural images represent bidimensional projections of the 3D world, and therefore they are intrinsecally characterized by near ideal object contours, which implies (at least in a statistical sense) high TAEC values. Instead, TEAC tends to diminish if edges are smeared (mainly because the magnitude ratio $\frac{\left|Y_{0,3}(x_1,x_2)\right|}{\left|Y_{0,1}(x_1,x_2)\right|}$ is smaller) and if edges are affected by disturbances or deviate irregularly (mainly due to phase coherence disruption).

Of course, the specific TAEC value does depend on the *specific image*. For this reason, we define the Relative TAEC (RTAEC) index as the ratio between the TAEC of the observed image and the TAEC of the original one:

$$RTAEC\left(I,\tilde{I}\right)=\frac{TAEC(I)}{TAEC(\tilde{I})}$$

The RTAEC index measures the TAEC quality gain of $I(x_1,x_2)$ with respect to $\tilde{I}(x_1,x_2)$. Its value is exactly 1 in the absence of quality modifications. It is <1 in case of degradation and >1 in case of improvement (occurring for instance in restoration or enhancement processes). Notice that, unlike most objective metrics, the RTAEC index is strictly *symmetric* by definition. In other words, changing the reference image with the observed one yields a reciprocal RTAEC value.

3.1 Contrast calibration

Prior to quality comparison, it could be required to remove from the observed images luminance and contrast mis-calibrations. In our case, luminance calibration is automatic, since mean grey level is ignored. As far as contrast is concerned, calibration can be performed, if desired, by previous normalization of the observed image with respect to the contrast ratio (CR) defined as:

$$CR\left(I,\tilde{I}\right)=\frac{\sum\left|\tilde{Y}_{0,1}(x_1,x_2)\right|^2}{\sum\left|Y_{0,1}(x_1,x_2)\right|^2}$$

This amounts to calculate the Normalized RTAEC defined as:

$$NRTAEC\left(I,\tilde{I}\right)=CR\left(I,\tilde{I}\right)\cdot RTAEC\left(I,\tilde{I}\right)$$

Therefore, the NRTAEC index requires one additional number for quality assessment.

4. EMPIRICAL TESTS

To conduct a preliminary validation of the proposed RTAEC index numerical empirical tests have been made on different images. A test consisted of comparing the RTAEC index values with the ones supplied by the state-of-art full reference MSSIM index [6] over the set of the images available in the Live Release 2 database (from the site http://live.ece.utexas.edu)

In Fig. 2 the scatter plot for each distortion source selected (Gaussian blur, additive white Gaussian noise, JPEG and JPEG2000 compression) are presented with reference to the available DMOS scores. Fig. 2(a) shows a much greater sensitivity of RTAEC over the MSSIM for blurred images. Fig 2(b) instead shows that MSSIM is more sensitive to additive noise. In any case, the RTAEC scores are generally consistent with the distortion level, except for images whose DMOS exceeds about 60. This corresponds to extremely corrupted images, outside the range of practical applications of RTAEC in its present formulation.

The scatter diagrams for JPEG and JPEG2000 compressed images are depicted in Figs. 2(c) and 2(d). In these cases, the combination of edge blur and coding artifacts leads to a RTAEC scatter versus DMOS globally similar to that exhibited by the MSSIM. The RTAEC confirms its high sensitivity to edge blur, evident in highly distorted JPEG2000 images. Again, outliers occurr for extremely corrupted images.

The following exemplary test refers to quality mesurements of images after resampling. In Fig. 3the quality of different spatial interpolation schemes is demonstrated using the RTAEC index. The original image “Einstein” (256 x 256 pixels) of Fig. 3(a) was resized to (128 x 128) using bicubic, bilinear and nearest neighbor pixel interpolation .In Figs. 3(b), 3(c) and 3(d) images are up-sampled by pixel repetition for display purposes. The bicubic interpolated image in Fig. 3(b) was taken as reference for quality

comparison. RTAEC results are consistent with expectation revealing high sensitivity to re-sampling artifacts.
Let us also remark that the RTAEC index is in principle insensitive to arbitrary image rotations and/or translations because it is based on rotation and translation invariant quantities. In a wider sense, it also tolerates moderate scaling and warping. In addition, the NRTAEC index is immune to contrast changes. These features may be useful for measuring the quality of projection devices.
Of course, non ideal re-sampling has great impact in the case of geometrical distortion. For instance, in Fig. 4a the re-sampling process causes a visible quality loss measured by a relatively low RTAEC value. As expected, this quality reduction is not present in the case of exact 90^0 rotation, as shown in Fig.4b. Notice that in the case of Fig. 4a the modest variation of the scanned surface does not introduce significant bias in the quality estimate.

Conclusive remarks

Compared to other metrics, the RTAEC index appears more sensitive to smearing than to noise. This behavior must be accounted for in quality assessment applications.

As far as computational aspects are concerned, convolutive operators for extracting angular harmonics are both cartesian separable (other than polar separable). Therefore, RTAEC is suited for computationally "fast" implementation.

Finally, let us remark that all what is needed for the RTAEC to be considered a No Reference (NR) index is the definition of a *conventional* TAEC reference value. In this perspective we argue that an absolute quality reference measure could be defined using the RTAEC with respect to specific contexts or stipulating some specific conditions. This is a matter of current work (along with application to color and video sequences).

REFERENCES

[1] S. Wolf, M.H. Pinson, "Low Bandwidth Reduced Reference Video Quality Monitoring System", *First International Workshop on Video Processing and Quality Metrics for Consumer Electronics*, Scottsdale, Arizona, January 23-25, 2005.
[2] Z. Whang E. Simoncelli : "Reduced-Reference Image Quality Assessment Using A Wavelet-Domain natural Image Statistic Model", *Human Vision and Electronic Imaging X, Proc. SPIE* 2005, vol. 5666.
[3] M.Carnec, P. Le Callet, D. Barba : " Visual Features for Image Quality Assessment with Reduced Reference," *Proc. of the IEEE ICIP* 2005, Vol.1, pp.421-424.
[4] G. Jacovitti, A. Neri, "Multiresolution circular harmonic decomposition," *IEEE Trans. on Signal Processing*, Vol. 48. No. 11, pp.3242-3247, November 2000.
[5] Z. Whang, E. Simoncelli : "Local Phase Coherence and the perception of Blur," *Advances in Neural Information processing Systems*, S.Thrun, L.Saul, and B. Scholkopf eds., Vol. 16, May 2004.
[6] Z. Wang, A. C. Bovik, H. R. Sheikh, and E. P. Simoncelli, "Image Quality Assessment: From Error Visibility to Structural Similarity," *IEEE Trans. on Image Processing*, Vol. 13, No. 4, pp. 600-612, April 2004.

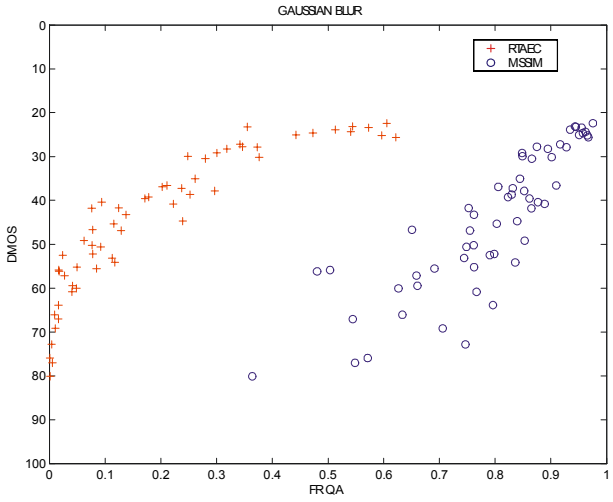

(a)

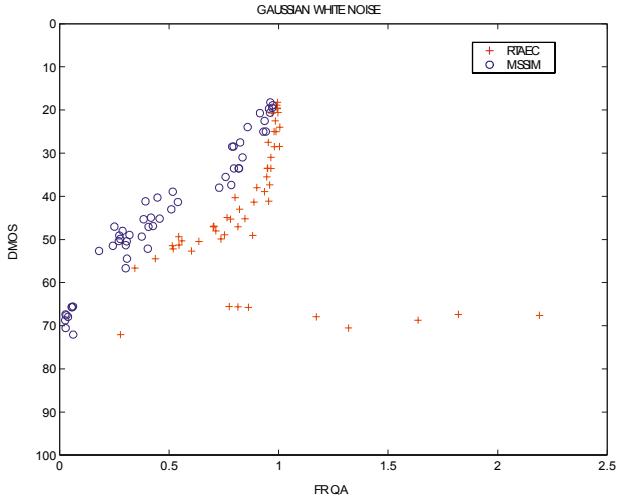

(b)

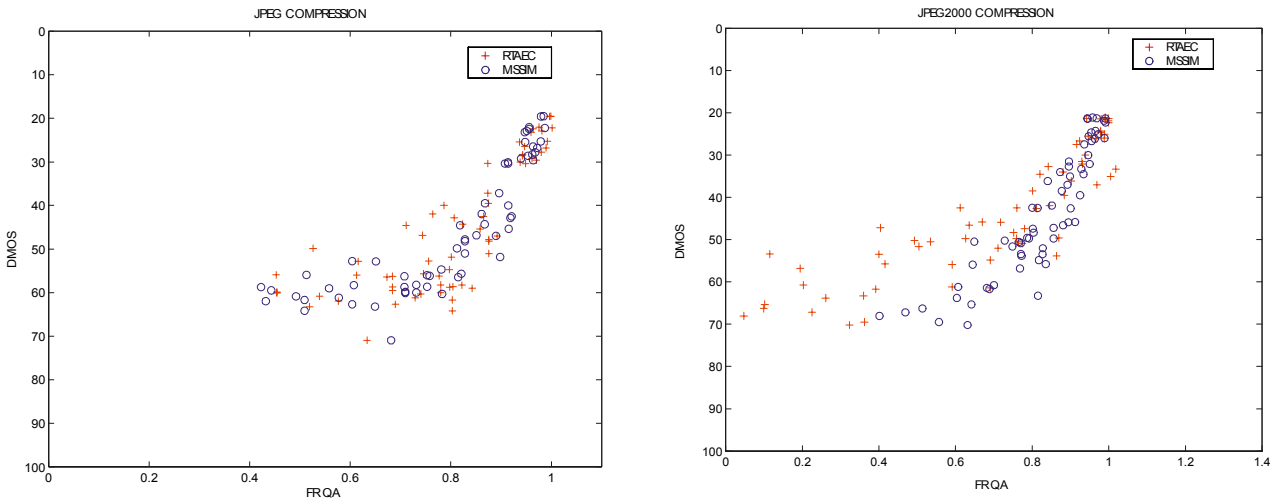

(c) (d)

Figure 2: Scatter diagrams for RTAEC and MSSIM versus the subjective DMOS for a subset of distorted images drawn from the Live Release 2 database (http://live.ece.utexas.edu/research/quality/subjective.htm). From left to right, top to bottom the diagrams show the results for the following distortions: (a) Gaussian blur, (b) White Gaussian noise; (c) JPEG, and (d) JPEG2000 compression.

(a) (b) (c) (d)

Figure 3: Images used for the RTAEC test for interpolation algorithms. (a) Original "Einstein" image (256 x 256 pixels); (b) Bicubic decimated image (128 x 128), considered as a reference for the other algorithms $RTAEC = 1.0$ **; (c) Bilinear interpolation** $RTAEC = 0.9090$ **; (d) Nearest neighbour pixel interpolation** $RTAEC = 0.5990$

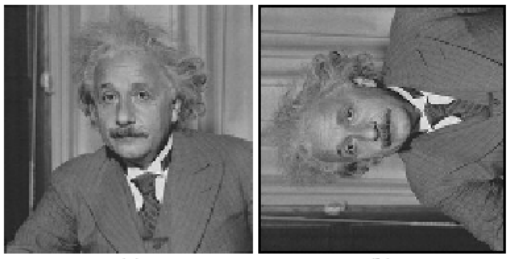

(a) (b)

Figure 4: (a), Bicubic decimated image (128 x 128) of a slightly rotated and expanded version of Fig. 3a Figure 4 (b) Bicubic decimated image (128 x 128) of a 90 ^{0} rotated version of Fig. 3a, $RTAEC = 1.0$